

Synthesis, Structure and Thermal Properties of Phosphophyllite, $\text{Zn}_2\text{Fe}(\text{PO}_4)_2 \cdot 4\text{H}_2\text{O}$

Ian M. Thomas and Mark T. Weller*

Department of Chemistry, The University of Southampton, Highfield, Southampton SO9 5NH, UK

Phosphophyllite, an important material in the coating of steels for rust prevention, has been synthesized in bulk from aqueous solution. A deuteriated sample has been studied by powder neutron diffraction and the structure refined in order to locate accurately the water molecule distribution. The thermal decomposition of this compound, studied by thermogravimetric and differential thermal analysis, is discussed in relation to its structure and its use as a precoat.

Keywords: Phosphophyllite; Neutron diffraction; Thermal analysis

Phosphophyllite, $\text{Zn}_2\text{Fe}(\text{PO}_4)_2 \cdot 4\text{H}_2\text{O}$, is one of a number of hydrated, first-row transition-metal phosphates that crystallize with a structure assembled from the metal ions in both octahedral and tetrahedral coordination and linked by phosphate tetrahedra. The compound occurs in nature and was first described by Laubmann and Steinmetz.¹ A number of X-ray crystallographic studies have subsequently been undertaken on naturally occurring samples^{2,3} with the definitive single-crystal X-ray study carried out by Hill.⁴ The compound crystallizes in the monoclinic space group $P2_1/c$ with $a = 10.378(3) \text{ \AA}$, $b = 5.084(1) \text{ \AA}$, $c = 10.553(3) \text{ \AA}$ and $\beta = 121.14(2)^\circ$ and may be described as consisting of $[\text{Zn}_2\text{P}_2\text{O}_7]$ tetrahedral sheets interleaved with $\text{FeO}_2 \cdot 4\text{H}_2\text{O}$ octahedral sheets. The structure is related to that of hopeite, $\text{Zn}_3(\text{PO}_4)_2 \cdot 4\text{H}_2\text{O}$,⁵ but in hopeite the linking of the various layers occurs in a different fashion. The structure of phosphophyllite is also related to that of *para*-hopeite⁶ through substitution of the octahedral zinc ions by the iron(II) ion. Hill was able to define in outline the positions of the hydrogen atoms from his X-ray refinement, though, obviously, using this technique they have large positional parameter errors and shortened O—H distances due to a shifted centre of diffraction for hydrogen attached to oxygen.

Phosphophyllite and hopeite are important materials with respect to their use as coatings for rust prevention.⁷ The phosphate coating typically consists of a mixture of the two phosphates, a higher phosphophyllite content being deemed desirable owing to its increased alkali resistance, which prevents its deterioration in the subsequent cationic electrodeposition of paint. The bath used to treat metal surfaces is usually iron free and iron is incorporated into the phosphate coating following dissolution from the substrate.

The thermal properties of the phosphate coating are also of critical importance. The curing of the paint applied to layers above the phosphate typically requires temperatures of 180°C . At these temperatures decomposition of the hydrated metal phosphates is possible though this process may be reversible. In the case of hopeite the effect of metal substitutions into the structure on the thermal properties has been investigated.⁸

In this paper we report the synthesis of bulk phosphophyllite and a structural study of a deuterated sample using powder neutron diffraction in order to clearly delineate the water molecule structure and hydrogen-bonding scheme. The thermal decomposition behaviour of phosphophyllite is also discussed in relation to the structure.

Experimental

Phosphophyllite was synthesized by adding a solution of diammonium hydrogen phosphate, $(\text{NH}_4)_2\text{HPO}_4$ (0.5 mol dm^{-3} , 30 cm^3) to a solution of zinc sulfate and iron(II) sulfate (total $[\text{M}^{2+}] = 0.5 \text{ mol dm}^{-3}$, 70 cm^3) with stirring. The resultant precipitate was left stirring for 4 h and then filtered using a grade 3 sintered glass crucible, washed with 1 dm^3 distilled water to remove excess sulfate, and then air-dried at 60°C . The total concentration of metal ions in the reaction was kept constant but their molar ratio was varied. With less than 40% iron in the reaction mixture hopeite was formed as well as phosphophyllite, but with 40% Fe^{2+} and above the mixed zinc/iron phosphate was the only product formed. Powder X-ray diffraction was used to identify the solids formed. The first reflection in the powder pattern for both hopeite and phosphophyllite occurs near $2\theta = 10^\circ$ for Cu-K α_1 radiation; these peaks occur with approximately equal intensities but with a separation of 0.3° . It is thus possible to determine the relative quantities of each phosphate in a mixture from the ratio of these peak intensities.

Synthesis of a deuteriated sample required a more complex route avoiding hydrogen-containing reactants. *Ca.* 12 g of FeCl_2 was prepared by passing $\text{HCl}(\text{g})$ over clean iron wire at 900°C for 6 h. The sample was transferred immediately to an inert dry atmosphere. Dried zinc chloride was used for the source of Zn^{2+} ions; ZnCl_2 hydrolyses in excess water therefore 13 g of ZnCl_2 was dissolved in the absolute minimum of D_2O (*ca.* 10 cm^3 , 98 atom% D). The FeCl_2 was also dissolved in 10 cm^3 D_2O and added to the ZnCl_2 solution, giving a molar iron:zinc ratio of *ca.* 50:50. $(\text{ND}_4)_2\text{HPO}_4$ is not commercially available necessitating its synthesis in the laboratory from D_3PO_4 and ND_4OD ; this solution was then added to the solution of metal ions with stirring. The resulting precipitate was filtered off, washed and dried using anhydrous ether. This process afforded *ca.* 4 g of $\text{Zn}_2\text{Fe}(\text{PO}_4)_2 \cdot 4\text{D}_2\text{O}$.

Powder neutron diffraction data were collected using the instrument D1A at the ILL, Grenoble. The sample was enclosed in a thin-walled vanadium can and data were collected over the angular range $0\text{--}160^\circ$ in 2θ during a period of 10 h. In order to reduce the thermal oscillations of the deuterium atoms as far as possible, the sample was cooled to 4 K in a vanadium-tailed cryostat. A wavelength of 2.988 \AA was chosen for the work in order to produce reasonably well resolved data at a high neutron flux. The background obtained over the angular range of the data was reasonably flat indicating a high level of deuteration in the sample.

The data were refined using the DBWS9600PC version of the Young and Wiles package.⁹ The initial starting model was taken from Hill;⁴ scattering lengths were taken as 0.568, 0.954, 0.513, 0.5807, 0.667×10^{-12} cm for Zn, Fe, P, O and D, respectively. Initial cycles of refinement were based around the profile parameters, scale-factor, zero-point, half-widths and background polynomial coefficients and resulted in an R_{wp} of ca. 30%. As the number of reflections was limited by the large wavelength used to collect the data it was decided not to refine the atom positions which had been defined accurately in the single-crystal study of Hill. Therefore, the only positional parameters refined were those of the deuterium atoms and these shifted significantly from the starting values. Temperature factors were set at reasonable values for the zinc, iron, phosphorous and oxygen atoms but allowed to refine for the deuterium atoms. However, values for the temperature factors of the three hydrogen-bonded deuterium atoms were constrained to the same value whilst that of the free deuterium, D(4), was allowed to vary independently. Final cycles of refinement involved 35 profile and atomic parameters. The concluding fit to the profile was excellent with $R_p = 3.96\%$, $R_{wp} = 4.83\%$ and $R_{exp} = 2.78\%$. Fig. 1 shows the final profile fit to the experimental data. A single weak peak that could not be indexed was observed at ca. 60° , indicating the presence of a small level impurity phase. With a single d -spacing the identification of this minor impurity was impossible.

Table 1 summarizes the final refined atomic positions and Table 2 derived bond distances and angles relevant to the refined portion of the structure. The temperature factors for the deuterium atoms are fairly large and probably reflect a

small amount of hydrogen exchange, reducing the effective scattering from these positions which would be ameliorated by the high thermal parameters.

Thermal decomposition of samples was carried out using a Stanton Redcroft TG1000 system and DTA 673-4 differential thermal analysis unit. Samples were heated at $10^\circ\text{C min}^{-1}$ in air. Infrared spectra were recorded from the as-synthesized $\text{Zn}_2\text{Fe}[\text{PO}_4]_2 \cdot 4\text{H}_2\text{O}$ and a sample heated to 200°C using a Perkin-Elmer FTIR.

Results and Discussion

Structure

The refined structure is presented in Fig. 2 showing the linking of the tetrahedral and octahedral elements and the hydrogen-atom positions. Final refined deuterium positions produce typical O—D bond lengths in both molecules in contrast to the values obtained by Hill in his X-ray diffraction study. Chiari and Ferraris¹⁰ have discussed the coordination geometry of water molecules in crystalline hydrates which have been studied by neutron diffraction. Water molecules in hydrates may be categorized into four classes depending on the nature of hydrogen-bonding patterns in which they take part. The two most common types occur in phosphophyllite: class 1, where only one of the two hydrogen atoms on a water molecule forms a hydrogen bond with the other free, and class 2, where both hydrogen atoms on a water molecule are engaged in the formation of hydrogen bonds. The D(1)—O(1)—D(2) molecule belongs to class 2 whilst D(3)—O(2)—D(4) belongs to class 1. Characteristic bond lengths in both these systems are discussed by Chiari and Ferraris and both water molecules in phosphophyllite are typical in terms of their bonding. If we consider the D(1)—O(1)—D(2) entity both deuteriums form hydrogen bonds to (different) O(3) atoms which link the phosphate tetrahedron to the FeO_6 octahedron. These interactions necessitate a fairly high D(1)—O(1)—D(2) bond angle of 116° . The D(3)—O(2)—D(4) molecule forms one strong hydrogen bond involving D(3) and the acceptor oxygen O(5) which links the zincate and phosphate tetrahedra; D(4) is non-hydrogen-bonded.

A comparison of the lattice parameters at room temperature and at 4 K show 0.95, 0.27 and 0.29% decrease in the a , b and c parameters, respectively, whilst β decreases slightly. The proportionately larger decrease in a which represents the layer separation is probably a result of the increased rigidity in the hydrogen bonds at the lower temperature decreasing the donor oxygen to acceptor oxygen ($\text{O}_a\text{—O}_d$) distances which lie mainly along a .

Thermal Properties

Fig. 3 shows the TG and DTA traces for phosphophyllite heated in air. Decomposition occurs in three stages. The initial weight loss in the range $100\text{--}200^\circ\text{C}$ corresponds to the loss of two water molecules yielding $\text{Zn}_2\text{Fe}[\text{PO}_4]_2 \cdot 2\text{H}_2\text{O}$. At higher temperatures, further decomposition occurs in a more complex two-stage process with the loss of the remaining two water molecules. The overall weight loss, 15.8%, is in excellent agreement with that expected for complete dehydration of the tetrahydrate, 16.04%. The initial formation of a dihydrate is similar behaviour to that seen for hopeite, though the thermal decomposition of this pure zinc phosphate seems to depend very much on the origin of the sample.⁵ A structural model has been proposed for the dihydrate formed from hopeite,¹¹ which involves selective loss of water molecules from the octahedrally coordinated zinc centres. It seems likely that a

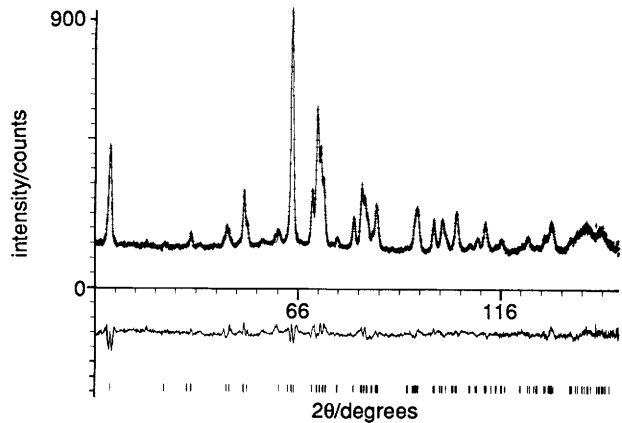


Fig. 1 Observed, calculated and difference plot for phosphophyllite. Tick marks show reflection positions

Table 1 Refined deuterium atomic coordinates for $\text{Zn}_2\text{Fe}[\text{PO}_4]_2 \cdot 4\text{D}_2\text{O}$; e.s.d.s are given in parentheses

atom	site	x	y	z	B
Fe	2	0.0	0.0	0.0	1.2
Zn	4	0.50024	0.31002	0.35464	1.1
P	4	0.68924	0.28707	0.19476	1.5
O(1)	4	−0.00460	0.29580	0.13926	1.2
O(2)	4	0.18030	0.28970	0.50308	1.2
O(3)	4	0.85429	0.25822	0.31583	1.2
O(4)	4	0.35262	0.07281	0.34204	1.2
O(5)	4	0.66173	0.13236	0.05825	1.2
O(6)	4	0.58607	0.15279	0.24452	1.2
D(1)	4	0.9487(13)	0.2704(27)	0.1987(15)	6.5(3)
D(2)	4	0.0584(17)	0.4574(26)	0.1595(15)	6.5(3)
D(3)	4	0.2376(15)	0.3732(38)	0.4734(18)	6.5(3)
D(4)	4	0.1940(14)	0.1119(37)	0.4929(15)	6.8(5)

space group $P2_1/c$; $a = 10.2797(8)$ Å, $b = 5.07021(1)$ Å, $c = 10.5224(4)$ Å, $\beta = 120.928(4)^\circ$.

Table 2 Determined bond lengths and angles relevant to the deuterium atoms in $\text{Zn}_2\text{Fe}[\text{PO}_4]_2 \cdot 4\text{D}_2\text{O}$; e.s.d.s are given in parentheses

atom	O _d	O _a	O _d —D	D—O _a	O _a —O _d	O _d —D—O _a	D—D	D—O—D
D(1)	O(1)	O(3)	0.973(15)	1.922(24)	2.891	174.2(1.0)	1.679(21)	116.9(1.5)
D(2)	O(1)	O(3)	0.998(15)	1.720(25)	2.712	172.7(1.0)		
D(3)	O(2)	O(5)	0.946(18)	1.772(29)	2.674	158.2(1.4)	1.455(36)	102.8(2.5)
D(4)	O(2)		0.915(18)					

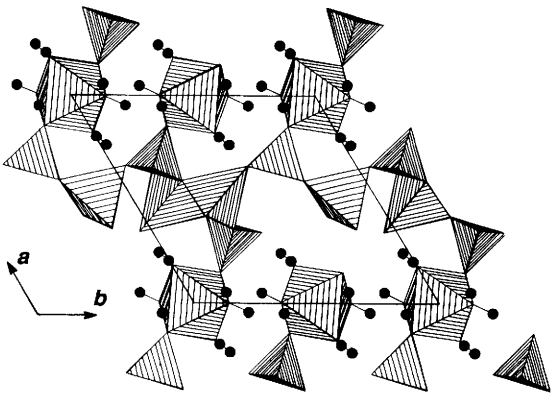


Fig. 2 Structure of phosphophyllite drawn using STRUPLO.¹² Refined deuterium positions are filled circles

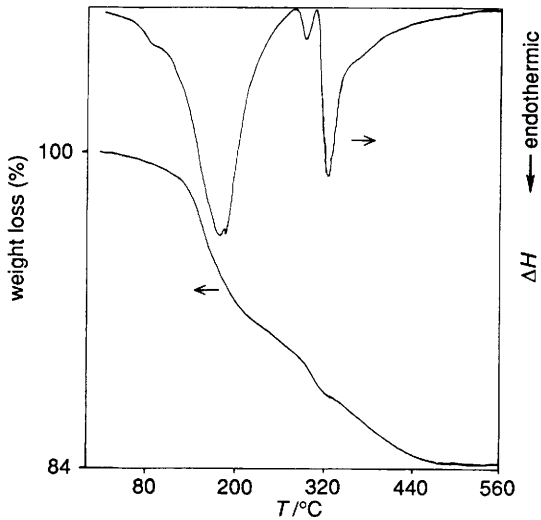


Fig. 3 Thermogravimetric (TG) and differential thermal analysis (DTA) curves for phosphophyllite in the temperature range 25–560 °C

similar process occurs with phosphophyllite. This is supported by the infrared data in relation to the structure of phosphophyllite.

The infrared spectra of $\text{Zn}_2\text{Fe}[\text{PO}_4]_2 \cdot 4\text{H}_2\text{O}$ and $\text{Zn}_2\text{Fe}[\text{PO}_4]_2 \cdot 2\text{H}_2\text{O}$ shown in Fig. 4 have complex absorption patterns in the OH stretching region. The OH stretching frequency of hydrogen-bonded hydrogen atoms has been directly related to the length and hence strength of the $\text{O}_d\text{H}—\text{O}_a$ interaction.¹² Formation of such interactions shifts the OH stretching frequency to lower frequencies and broadens the absorption. The OH stretching frequency therefore correlates well with the $\text{O}_a—\text{O}_d$ distance. This allows assignment of the various absorptions in the OH stretching region to particular OH moieties in the compound as summarized in Table 3. The sharp peak at 3570 cm^{-1} can, therefore, clearly be assigned to $\text{O}(2)—\text{D}(4)$.

Heating the sample to 200 °C results in a marked change in the infrared spectrum. Of most note is the disappearance of the sharp peak implying the loss of $\text{O}(2)—\text{D}(4)$. This is as

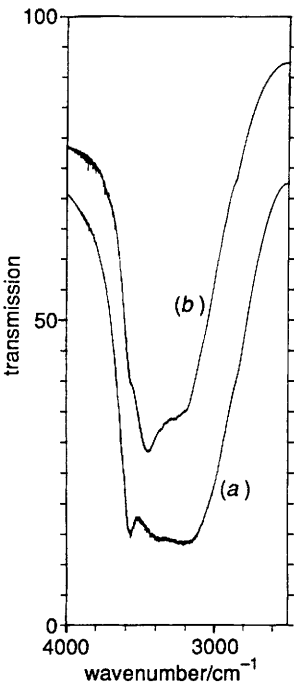


Fig. 4 Infrared spectra of (a) $\text{Zn}_2\text{Fe}[\text{PO}_4]_2 \cdot 4\text{H}_2\text{O}$ (b) $\text{Zn}_2\text{Fe}[\text{PO}_4]_2 \cdot 2\text{H}_2\text{O}$ in the OH stretching region

Table 3 OH stretching frequencies and assignments for $\text{Zn}_2\text{Fe}[\text{PO}_4]_2 \cdot 4\text{H}_2\text{O}$

experimental/ cm^{-1}	assignment
3570	$\text{O}(2)—\text{D}(4)$
3395	$\text{O}(1)—\text{D}(1)$
3220	$\text{O}(2)—\text{D}(3)$, $\text{O}(1)—\text{D}(2)$

expected if the $\text{D}(3)—\text{O}(2)—\text{D}(4)$ water molecule is lost from the structure. As this water molecule is less strongly bound in the cell then it is likely that it would be lost in preference to $\text{D}(1)—\text{O}(1)—\text{D}(2)$. The positions of the remaining OH absorptions indicate that the remaining water molecule is still hydrogen bonded in the dihydrate structure, but probably less strongly with OH stretching frequencies at *ca.* 3400 cm^{-1} .

In hopeite replacement of zinc by smaller transition-metal ions and magnesium⁸ causes the decomposition temperature to shift to higher values. These substitutions reduce the lattice parameter and may produce stronger hydrogen bonding in the structure by contracting the $\text{O}_a—\text{O}_d$ distances. It is possible, therefore, that similar substitutions in the phosphophyllite structure would allow shortening of the $\text{O}(2)—\text{O}(5)$ distance holding the $\text{D}(3)—\text{O}(2)—\text{D}(4)$ more strongly in the lattice and increasing the phosphophyllite decomposition temperature.

We thank SERC and ICI Paints Division for the support of a CASE studentship for I.M.T.

References

- 1 H. Laubmann and H. Steinmetz, *Z. Kryst. Mineral.*, 1920, **55**, 523.
- 2 F. Liebau, *Chem. Erde.*, 1962, **22**, 430.
- 3 F. Liebau, *Acta Crystallogr.*, 1965, **18**, 352.
- 4 R. J. Hill, *Am. Mineral.*, 1977, **62**, 812.
- 5 R. J. Hill and J. B. Jones, *Am. Mineral.*, 1976, **61**, 987.
- 6 G. Y. Chao, *Z. Krist.*, 1969, **130**, 261.
- 7 T. Yoshihara and H. Okita, *Trans. ISIJ.*, 1983, **23**, 984.
- 8 S. Haussühl, B. Middendorf and M. Dörffel, *J. Solid State Chem.*, 1991, **93**, 9.
- 9 D. B. Wiles and R. A. Young, *J. Appl. Crystallogr.*, 1981, **14**, 149.
- 10 G. Chiari and G. Ferraris, *Acta Crystallogr. Sect. B*, 1982, **38**, 2331.
- 11 E. Sahakian and Y. Arnaud, *C.R. Acad. Sci. Paris*, 1988, **306**, 277.
- 12 R. Fischer, *J. Appl. Crystallogr.*, 1985, **18**, 258.

Paper 2/03707F; Received 13th July, 1992